Impact of Tube-to-Particle-Diameter Ratio on Pressure Drop in Packed Beds

M. Winterberg and E. Tsotsas
Thermal Process Engineering, Otto-von-Guericke-University Magdeburg, Universitätsplatz 2, D-39106 Magdeburg, Germany

Packed tubes are frequently used in industry as heat exchangers, adsorbers, or chemical reactors. For the design and operation of such equipment the pressure drop in packed beds with fluid flow must be known. After decades of intensive research it is generally accepted that the pressure drop can be calculated by simple, semiempirical models like the Ergun equation (Ergun, 1952) in a satisfactory way, at the limit of an infinitely extended packed bed. However, uncertainties still exist for packed tubes with low and medium values of tube-to-particle-diameter ratio D/d_p. In this case, the increased porosity of the bed near the wall results in an increased permeability and flow maldistribution. Additionally, the viscous friction at the wall may not be negligible in comparison to that caused by the particles.

Various authors address the issue of pressure drop in spatially constrained packed beds. Mehta and Hawley (1969) as well as Brauer (1971) have tried to describe the wall effect by taking the surface area of the tube into account in the definition of the hydraulic diameter. In a more recent work Cohen and Metzner (1981) calculate pressure drops by subdividing the cross section into three regions, assuming that the relative spatial extent of each region depends on the tube-to-particle-diameter ratio D/d_p. Nield (1983) proposes a similar model with two regions. Chu and Ng (1989) have developed quite a sophisticated pore simulation, and carry out measurements at low Reynolds numbers. Sodré and Parise (1997) calculate the pressure drop in an annular bed of spheres by subdivision into, again, three regions. Detailed surveys of older literature are given by Brauer (1971) and Cohen and Metzner (1981).

Of special interest in this context is the work of Chu and Ng (1989) and the subsequent discussion by Tsotsas and Schlünder (1990). This discussion clarified that the primary impact of spatial constraint is an increase of average bed porosity $\overline{\psi}$ in respect to the porosity of the infinitely extended bed ψ_∞. Applying the Ergun equation for these porosities, a pressure drop Δp_{hom} (at $\overline{\psi}$) is obtained that can be considerably lower than the pressure drop Δp_∞ (at ψ_∞). Since $\overline{\psi}$ and Δp_{hom} are easily accessible, the remaining problem is to derive the quotient of the actual pressure drop Δp to the reference value Δp_{hom} for varying diameter ratio, that is, to find the function $\Delta p/\Delta p_{\mathrm{hom}}(D/d_p)$. A satisfactory solution of this problem could not be offered in 1990, so a number of questions remain open, concerning:

- The extent of the impact of flow maldistribution or wall friction on $\Delta p/\Delta p_{\mathrm{hom}}$, when considered separately;
- The direction ($\Delta p/\Delta p_{\mathrm{hom}} \lesseqgtr 1$) of the combined impact of flow maldistribution and wall friction, including the possibility of inversion (that is, of an intersection of the function $\Delta p/\Delta p_{\mathrm{hom}}(D/d_p)$ with the line $\Delta p/\Delta p_{\mathrm{hom}} = 1$, as suggested by Chu and Ng (1989));
- The extent of the combined impact in respect to practical requirements of accuracy and its experimental detectability.

The present contribution tries to answer these questions on the basis of the extended Brinkman equation that enables the calculation of macroscopic flow profiles in packed tubes by consideration of both the lateral porosity profile and the wall friction. This approach can be followed back to the 1980s (such as Vortmeyer and Schuster, 1983), but attained maturity only recently by successes in the description of measured velocity profiles (Giese et al., 1998; Bey and Eigenberger, 1997), catalytic reaction (Vortmeyer and Haidegger, 1991; Hein, 1998), and heat and mass transfer (Winterberg et al., 1998, 2000). To our knowledge, no systematic evaluation of pressure drop is available until now. After specifying the model, calculated $\Delta p/\Delta p_{\mathrm{hom}}(D/d_p)$ functions will be presented, discussed, and recapitulated in the form of conclusions.

The Model

Referring to practical applications like heterogeneous catalysis or adsorption, subsequent analysis will be restricted to cylindrical tubes, filled with particles that are nearly (but not perfectly) monodispersed in size and nearly (but not perfectly) spherical in shape. For these conditions the monotonic exponential expression after Giese (1998)

$$\psi(r) = \psi_\infty\left(1 + 1.36\exp\left[-5.0\frac{R-r}{d_p}\right]\right), \qquad (1)$$

with $\psi_\infty = 0.37$, will be used to calculate radial porosity profiles $\psi(r)$, as was already done by Hein (1998) and Winter-

berg et al. (1998, 2000) (see earlier). Equation 1 agrees very well with experimental results by Giese (1998) for real catalyst beds. Similar porosity functions have been applied by Vortmeyer and Schuster (1983), among others.

The extended Brinkman equation is written in the one-dimensional form

$$\frac{\partial p}{\partial z} = - f_1 u_0(r) - f_2 \left[u_0(r) \right]^2 + \frac{\eta_{\text{eff}}}{r} \frac{\partial}{\partial r} \left(r \frac{\partial u_0(r)}{\partial r} \right), \quad (2)$$

with

$$f_1 = 150 \frac{(1-\psi(r))^2}{\left[\psi(r)\right]^3} \frac{\eta_f}{d_p^2} \qquad \text{and}$$

$$f_2 = 1.75 \frac{(1-\psi(r))}{\left[\psi(r)\right]^3} \frac{\rho_f}{d_p} \quad (3)$$

and the boundary conditions

$$r = 0 \rightarrow \frac{\partial u_0}{\partial r} = 0, \quad (4)$$

and

$$r = R \rightarrow u_0 = 0; \quad (5)$$

compare with Chandrasekhara and Vortmeyer (1979) and Vortmeyer and Schuster (1983). The first two terms on the righthand side of Eq. 2 account for the head loss caused by the particles and are widely known as the D'Arcy and quadratic or Ergun term, respectively. The third term describes the head loss resulting from viscous friction in the vicinity of the wall and combines with the nonslip boundary condition of Eq. 5.

Giese et al. (1998) used LDA to investigate the velocity distribution in packed beds of very regular, uniformly sized glass particles of four different shapes. For every shape (perfect spheres, deformed spheres, cylinders, and Raschig rings), they could describe their measurements successfully with Eqs. 2 to 5 by fitting the effective viscosity η_{eff}. Measurements with real catalyst particles (imperfect spheres with a certain size dispersity), which would correspond exactly to the porosity profile of Eq. 1, are not available. In this situation, it appears appropriate to use the η_{eff} from Giese et al. (1998) that can reasonably be assumed to combine at best with Eq. 1, namely

$$\frac{\eta_{\text{eff}}}{\eta_f} = 2.0 \cdot \exp\left(2.0 \times 10^{-3} Re_0\right) \quad (6)$$

for their deformed spheres. Here the Reynolds number Re_0 is defined as

$$Re_0 = \frac{\bar{u}_0 \rho_f d_p}{\eta_f}, \quad (7)$$

with the average superficial velocity

$$\bar{u}_0 = \frac{2}{R^2} \int_0^R u_0(r) r \, dr. \quad (8)$$

The combination of Eq. 6 with Eq. 1 is consistent with the successful analysis of heat transfer, mass transfer, and catalytic reaction by Hein (1998) and Winterberg et al. (1998, 2000). Exchanging Eq. 1 with a moderately oscillating function [such as after figure 2b of Giese et al. (1998)] does not substantially change the results of the present work on pressure drop, as respective calculations have shown. To be sure, further LDA measurements under systematic variation of particle sphericity, particle size dispersity, and Reynolds number are necessary in order to completely clarify the issue. Such investigations might also shed light on further questionable aspects of Eq. 6, like its limiting behavior ($\eta_{\text{eff}} = 2\eta_f$ for $Re_0 \rightarrow 0$) and the independence of η_{eff} from radial position.

In the present work, solutions of Eq. 2—that is, values of the pressure drop per unit length—are derived numerically with the help of the subroutine D02RAF of the NAG Fortran Library (1993). This tool uses the deferred-correction technique and Newton iteration to solve a two-point boundary-value problem with general boundary conditions for a system of ordinary differential equations. The adaptive meshes are automatically produced. The numerical method is described in detail by Lentini and Pereyra (1977).

Three kinds of pressure drop have been calculated in this way:

- The pressure drop Δp_c corresponding to the complete set of Eqs. 1 to 5, and thus accounting for the impact of both the wall friction and radial distribution of porosity and flow velocity;
- The pressure drop Δp_w including only the influence of the wall friction model, that is, with $\psi(r) = \bar{\psi}$ for every radial position;
- The pressure drop Δp_m considering only the maldistribution of porosity and flow, that is, with $\psi(r)$ from Eq. 1 and respective $u_0(r)$ profiles, but without wall friction ($\eta_{\text{eff}} = 0$).

Additionally, both wall friction and maldistribution are neglected ($\eta_{\text{eff}} = 0$, $\psi(r) = \bar{\psi}$, $u_0(r) = \bar{u}_0$) in order to obtain the reference value of Δp_{hom}, as discussed at the beginning of the note. In any case, the average porosity $\bar{\psi}$, which depends on the tube-to-particle-diameter ratio D/d_p, is calculated from Eq. 1 by integration. The quantities Δp_w and Δp_m define, in a sense, limiting cases of the problem without necessarily constituting an envelope for Δp_c, as we will see later on. Every calculated pressure drop is referred to Δp_{hom}, leading to values of the function $\Delta p / \Delta p_{\text{hom}}(D/d_p)$.

Results and Discussion

Calculated pressure drops are depicted in Figures 1 and 5 for different effective viscosities ($\eta_{\text{eff}} = \eta_f$, Figure 1, respectively, η_{eff} acc. to Eq. 6, Figure 5), two Reynolds numbers ($Re_0 = 1$, respectively, $Re_0 = 1000$) containing the entire range of practical relevance, and a variation of D/d_p from 4 to 40. Since flow computation in every single void of the bed would be more appropriate than the present approach at $D/d_p < 4$, such values have not been considered. Beds with $D/d_p > 40$ can be regarded as infinitely extended. Results of the complete model (solid lines, Δp_c; see earlier) are plotted together with results with only maldistribution (broken lines, Δp_m, "maldistribution model") and numerical data with only wall friction (broken/dotted lines, Δp_w, "wall friction model").

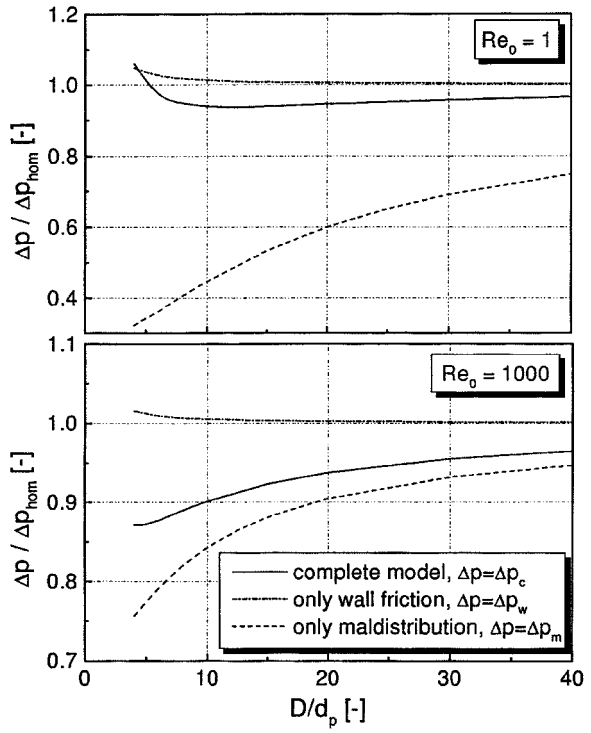

Figure 1. Influence of diameter ratio D/d_p on reduced pressure drop $\Delta p/\Delta p_{hom}$ for two different Reynolds numbers; $\Delta p/\Delta p_{hom}$ calculated with $\eta_{eff} = \eta_f$.

Figure 1 shows the expected trend for the maldistribution model: the reduced pressure drop $\Delta p_m/\Delta p_{hom}$ decreases with decreasing tube-to-particle-diameter ratio so it is always smaller than unity. Consequently, maldistribution alone is favorable in terms of pressure drop. This behavior is quite general and easy to understand, since the combination of resistances in parallel is always smaller than the corresponding average resistance. Low Reynolds numbers and diameter ratios enhance channeling, and thus enforce this effect. The wall-friction model shows opposite behavior. There, pressure drop is always larger than the reference value ($\Delta p_w > \Delta p_{hom}$), though not very significantly. The quotient $\Delta p_w/\Delta p_{hom}$ decreases with increasing D/d_p. The results of the complete model emphasize that the superposition of the effects of maldistribution and wall friction is complex and extremely nonlinear. The resulting $\Delta p_c/\Delta p_{hom}$ curve can have increasing or decreasing parts, a minimum and an inflection point. An intersection with the line $\Delta p/\Delta p_{hom} = 1$ is possible at a D/d_p value that increases with decreasing Reynolds number. Consequently, the reference value of Δp_{hom} may be outranged or undercut by the actual pressure drop, depending on operating conditions. Even an intersection with the $\Delta p_w/\Delta p_{hom}$ curve is possible, though this occurs only at a low Reynolds number and for a D/d_p quotient in the vicinity of 4. This means that wall friction, combined with flow maldistribution, may inhibit the flow more strongly than by itself. Remember that Figure 1 has been calculated by simply setting the effective viscosity η_{eff} equal to the viscosity of the fluid η_f.

The findings of Figure 1 may be elucidated by observing the corresponding velocity profiles. These profiles are depicted for all three model variants and $D/d_p = 4$ in Figure 2 ($Re_0 = 1$) and Figure 3 ($Re_0 = 1000$). Due to the invariance of Re_0, all profiles shown in one and the same plot have the same average ($\bar{u}_0$). As already pointed out, the model with only maldistribution automatically delivers a velocity profile that is optimal in terms of overall permeability. As Figure 3 shows, the velocity profile according to the complex model does not deviate very much from the optimum at $Re_0 = 1{,}000$. Therefore, the respective value of $\Delta p_c/\Delta p_{hom}$ at $D/d_p = 4$ in Figure 1 (solid line) is not very far from the value $\Delta p_m/\Delta p_{hom}$ at the same D/d_p and is considerably lower than unity. In contrast, for $Re_0 = 1$ (Figure 2) large differences occur between the velocity profiles of the complete and the maldistribution model. In other words, real flow is distributed, due to wall friction, in a way that is clearly not optimal in terms of resistance minimization. Consequently, a much stronger pressure-drop increase is observed in Figure 1 at $Re_0 = 1$, and the quotient $\Delta p_c/\Delta p_{hom}$ is larger than unity for $D/d_p = 4$. A duality in the impact of wall friction becomes evident. In this

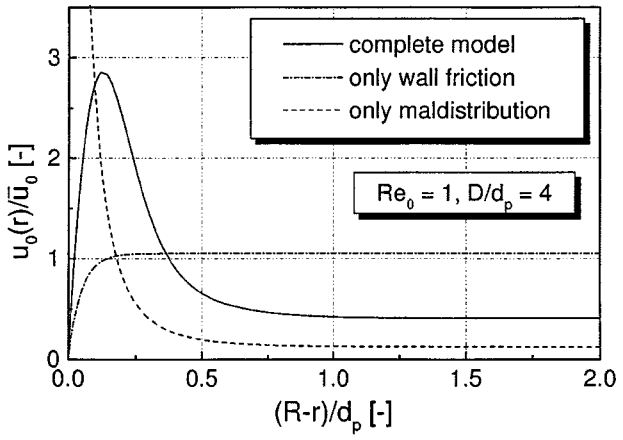

Figure 2. Reduced-velocity profiles corresponding to Figure 1 ($\eta_{eff} = \eta_f$) for $Re_0 = 1$, $D/d_p = 4$; the value u_0 ($r = R$) of the maldistribution model is large, but finite.

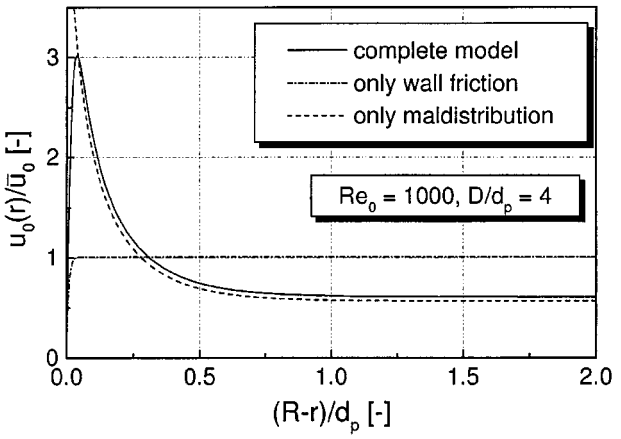

Figure 3. Reduced-velocity profiles corresponding to Figure 1 ($\eta_{eff} = \eta_f$) for $Re_0 = 1{,}000$, $D/d_p = 4$.

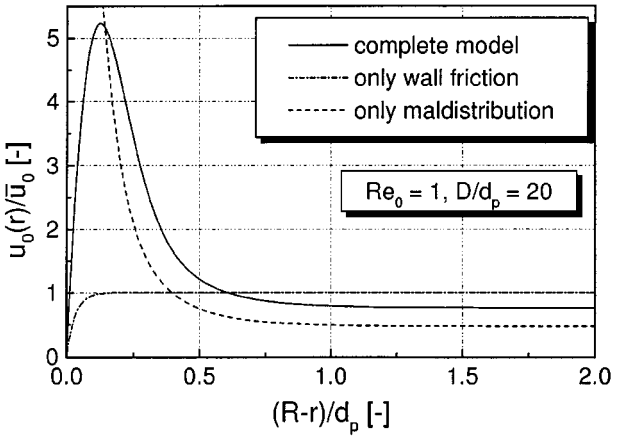

Figure 4. Reduced-velocity profiles corresponding to Figure 1 ($\eta_{eff} = \eta_f$) for $Re_0 = 1$, $D/d_p = 20$.

duality, the direct wall friction treated, for example, in Mehta and Hawley (1969) or Brauer (1971), by linearly combining tube and particle surface area is only one aspect. The second, potentially more important aspect is the radial shift of the velocity profiles that results from the fulfillment of the non-slip boundary condition at the wall, thus forcing fluid elements to pass through regions of decreased porosity that otherwise would have been avoided. No hydraulic diameter concept is able to describe this complex interaction. The behavior of the velocity profiles in Figure 4 ($Re_0 = 1$, $D/d_p = 20$) is placed somewhere between that of Figure 2 and Figure 3, and the same is true for the respective $\Delta p_c/\Delta p_{hom}$ value of the complete model in Figure 1.

Figure 5 contains the pressure-drop ratios $\Delta p/\Delta p_{hom}$ calculated with the effective viscosity η_{eff} according to Eq. 6. As already discussed, and in spite of still existing limitations (see the opening paragraphs and the model section), several arguments indicate that the plot of Figure 5 may reflect the reality more closely than does Figure 1, and for practical purposes be an appropriate recommendation. In mathematical terms, the only difference between Figure 5 and Figure 1 is that the effective viscosity has been increased ($\eta_{eff}/\eta_f > 1$, acc. to Eq. 6) and depends on Re_0. Predictions of the maldistribution model are not influenced by this fact, so the $\Delta p_m/\Delta p_{hom}$ curves remain the same. As expected, larger values of $\Delta p_w/\Delta p_{hom}$ are predicted by the wall friction model in Figure 5. Furthermore, the predictions of the complete model (solid $\Delta p_c/\Delta p_{hom}$ curves) are shifted considerably toward the upper right corner of the plot. In this way, intersection points with the line $\Delta p/\Delta p_{hom} = 1$ and the $\Delta p_w/\Delta p_{hom}$ curve occur for both Reynolds numbers at relatively high values of D/d_p (at $D/d_p \approx 20$, respectively, $D/d_p \approx 13$ for $Re_0 = 1$). Furthermore, the impact of channeling is almost wiped out, so that pressure drops lie up to 20% over the reference value at small D/d_p ratios and undercut only marginally Δp_{hom} at large values of D/d_p. This may explain why the older literature concentrates on some additive, inhibiting overall influence of the wall. This conforms with the interpretation of the trend of existing data by Tsotsas and Schlünder (1990).

Figure 6 shows typical velocity profiles corresponding to the calculations of Figure 5 for $D/d_p = 4$ and $Re_0 = 1$. The viscous wall friction has a greater influence than in Figure 2

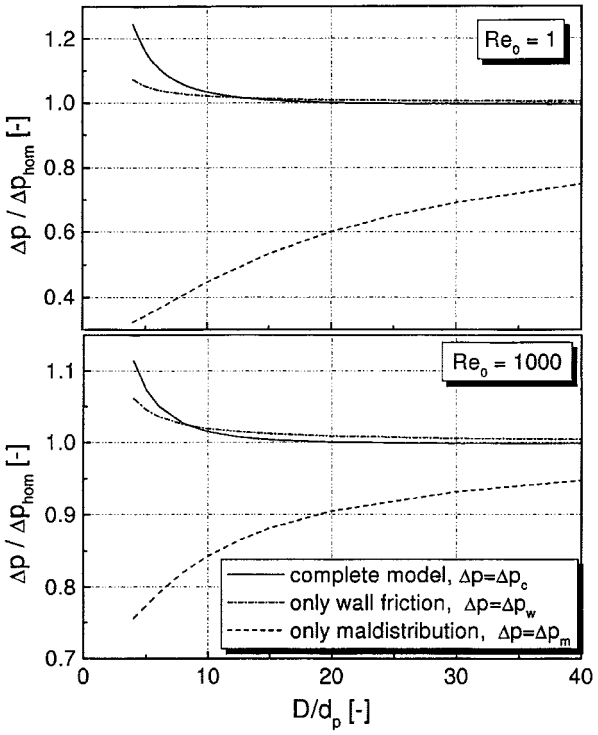

Figure 5. Influence of diameter ratio D/d_p on reduced pressure drop $\Delta p/\Delta p_{hom}$ for two different Reynolds numbers; $\Delta p/\Delta p_{hom}$ calculated with η_{eff} after Eq. 6.

because of the larger value of the effective viscosity η_{eff}. This can be seen, for example, in the profile of the wall friction model, which has a larger velocity in the core of the bed. The same profile shows that the frictional impact of the wall is still short-ranged, which may justify the separation of η_{eff} from r in the approach by Giese et al. (1998). In comparison to the calculation with $\eta_{eff} = \eta_f$ of Figure 2 the curve of the complete model shows a less pronounced maximum, a higher core velocity, and a stronger deviation from the results of the maldistribution model. All these factors favor a larger pres-

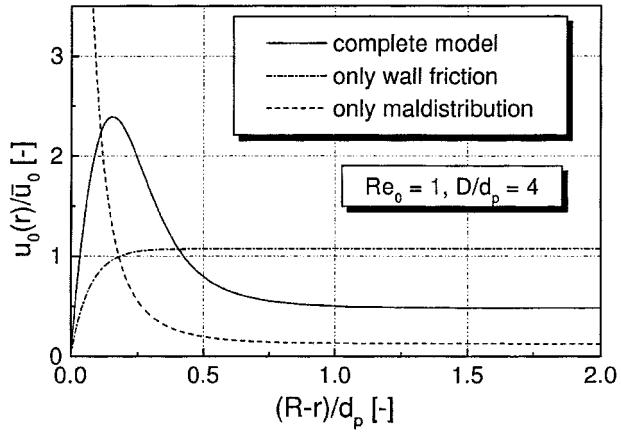

Figure 6. Reduced-velocity profiles corresponding to Figure 5 (η_{eff} after Eq. 6) for $Re_0 = 1$, $D/d_p = 4$.

sure drop and agree well with the comparison of Figure 5 to Figure 1.

From a practical point of view, Figure 5 emphasizes the applicability of the Ergun equation with $\bar{\psi}$, $\bar{u}_0$ (of Δp_{hom}) down to quite small tube-to-particle-diameter ratios D/d_p. Actually, the difference between the predictions of the complete model and Δp_{hom} is smaller than 3%, which means it lies beyond measurability or practical relevance for $D/d_p > 10$. In the region $10 > D/d_p > 4$ increasing deviations are observed that depend on the exact value of D/d_p and on the Reynolds number and may reach +20%, which is relevant in practical terms. The present analysis, similar overall trends with previous hydraulic diameter considerations, and its success in other applications indicate that the model of Giese et al. (1998) is likely to be the right choice for practical pressure drop calculations within this range. It should be stressed, however, that a final choice between Figure 5 and Figure 1 (that is, a final conclusion on the existence and value of the effective viscosity η_{eff}) would require a comprehensive validation with experimental data and is outside the scope of the present communication. Data from the literature may not be adequate for this purpose in terms of both documentation and accuracy (such as the large impact of $\bar{\psi}$ on the reference value Δp_{hom}). Nevertheless, conditions favorable for differentiation can well be derived from the present analysis, namely as regions or points of maximal deviation between the solid lines of Figure 5 and Figure 1. Thus, a combination of pressure drop measurements with LDA flow-field determination may provide a final insight.

Conclusion

Discussions in the literature about the influence of (1) the operating parameters Re_0 (Reynolds number) and D/d_p (tube-to-particle-diameter ratio), and (2) the physical phenomena of wall friction and flow maldistribution on the pressure drop in packed tubes are in conflict. This influence is analyzed by applying the extended Brinkman equation to cylindrical beds of particles of nearly (but not perfectly) spherical shape and moderate-size dispersity. In all cases, the calculated pressure drop is compared with the value Δp_{hom}, which is obtained by the Ergun equation for the average bed porosity, $\bar{\psi}$, and superficial velocity, $\bar{u}_0$. The main conclusions of the study are as follows:

- Maldistribuion alone can significantly decrease pressure drop with respect to Δp_{hom}, while wall friction alone increases it moderately.
- The combination of both effects in the complete model is extremely nonlinear, leading to ratios of $\Delta p/\Delta p_{\text{hom}}$ that may be smaller, equal to, or larger than unity, depending on D/d_p, Re_0, and the effective viscosity η_{eff}. This complex interaction, which is also reflected to the velocity profiles, cannot be described by simplified approaches.
- Effective viscosities after Giese et al. (1998)—Eq. 6—deliver pressure drops that are almost identical to Δp_{hom} for $D/d_p > 10$. For $10 > D/d_p > 4$, practically significant deviations from Δp_{hom} up to +20% are possible. Very small diameter beds ($D/d_p < 4$) have not been considered.
- While lingering uncertainties about the effective viscosity η_{eff} require additional experimental investigation, the results of the present study may be helpful in focusing future work.

Acknowledgment

The present work has been funded by the Deutsche Forschungsgemeinshaft (DFG).

Notation

R = tube radius
r = radial coordinate, m
u_0 = local superficial velocity, m/s
z = axial coordinate, m
η = dynamic viscosity, Pa·s
ρ = density, kg/m^3
ψ = local bed porosity

Subscripts

f = fluid
hom = homogeneous model

Literature Cited

Bey, O., and G. Eigenberger, "Fluid Flow Through Catalyst Filled Tubes," *Chem. Eng. Sci.*, **52**, 1365 (1997).
Brauer, H., *Grundlagen der Einphasen und Mehrphasenströmungen*, Sauerländer Verlag, Aarau/Frankfurt (1971).
Chandrasekhara, B. C., and D. Vortmeyer, "Flow Model for Velocity Distributions in Fixed Beds under Isothermal Conditions," *Wärme-Stoffübertrag.*, **12**, 105 (1979).
Chu, C. F., and K. M. Ng, "Flow in Packed Bed Tubes with Small Tube to Particle Diameter Ratio," *AIChE J.*, **35**, 148 (1989).
Cohen, Y., and A. B. Metzner, "Wall Effects in Laminar Flow of Fluids Through Packed Beds," *AIChE J.*, **27**, 705 (1981).
Ergun, S., "Fluid Flow Through Packed Columns," *Chem. Eng. Progr.*, **48**, 89 (1952).
Giese, M., "Strömung in porösen Medien unter Berücksichtigung effektiver Viskositäten," PhD Diss., Technical University, München, Germany (1998).
Giese, M., K. Rottschäfer, and D. Vortmeyer, "Measured and Modelled Superficial Flow Profiles in Packed Beds with Liquid Flow," *AIChE J.*, **44**, 484 (1998).
Hein, S., "Modellierung wandgekühlter katalytischer Festbettreaktoren mit Ein- und Zweiphasenmodellen," PhD Diss., Technical University, München, Germany (1998).
Lentini, M., and V. Pereyra, "An Adaptive Finite Difference Solver for Nonlinear Two-Point Boundary Problems with Mild Boundary Layers," *SIAM J. Numer. Anal.*, **14**, 91 (1977).
Mehta, D., and M. C. Hawley, "Wall Effects in Packed Columns," *Ind. Eng. Chem. Proc. Des. Dev.*, **8**, 280 (1969).
NAG Fortran Library, Mark 16, Oxford (1993).
Nield, D. A., "Alternative Model for Wall Effect in Laminar Flow of Fluid Through a Packed Column," *AIChE J.*, **29**, 688 (1983).
Sodré, J. R., and J. A. R. Parise, "Fluid Flow Pressure Drop Through an Annular Bed of Spheres with Wall Effects," *Exp. Therm. Fluid Sci.*, **17**, 265 (1997).
Tsotsas, E., and E. U. Schlünder, "The Influence of Tube to Particle Diameter Ratio on Pressure Prop in Packed Tubes: Remarks on a Recent Paper by Chu and Ng," *AIChE J.*, **36**, 151 (1990).
Vortmeyer, D., and E. Haidegger, "Discrimination of Three Approaches to Evaluate Heat Fluxes for Wall-Cooled Fixed Bed Chemical Reactors," *Chem. Eng. Sci.*, **46**, 2651 (1991).
Vortmeyer, D., and J. Schuster, "Evaluation of Steady Flow Profiles in Rectangular and Circular Packed Beds by a Variational Method," *Chem. Eng. Sci.*, **38**(10), 1691 (1983).
Winterberg, M., E. Tsotsas, A. Krischke, and D. Vortmeyer, "Wärmetransport und chemische Reaktion in durchströmten Festbetten—Eine Neuevaluierung," *Chem. Ing. Tech.*, **70**, 1094 (1998).
Winterberg, M., E. Tsotsas, A. Krischke, and D. Vortmeyer, "A Simple and Coherent Set of Coefficients for Modelling of Heat and Mass Transport With and Without Chemical Reaction in Tubes Filled With Spheres," *Chem. Eng. Sci.*, **55**, 967 (2000).

Manuscript received Feb. 4, 1999, and revision received Oct. 15, 1999.